Astron. Astrophys. 290, 324–334 (1994)

ASTRONOMY AND ASTROPHYSICS

Solar radiation pressure perturbations for Earth satellites

III. Global atmospheric phenomena and the albedo effect

D. Vokrouhlický [1,2], P. Farinella [3,4], and F. Mignard [2]

[1] Astronomical Institute, Charles University, Švédská 8, 15000 Prague 5, Czech Republic
[2] Observatoire de la Côte d'Azur, Dept. CERGA, URA CNRS 1360, Av. N. Copernic, F-06130 Grasse, France
[3] Dipartimento di Matematica, Università di Pisa, Via Buonarroti 2, I-56127 Pisa, Italy
[4] Observatoire de la Côte d'Azur, Dept. Cassini, URA CNRS 1362, B.P. 229, F-06304 Nice, France

Received 8 February 1994 / Accepted 28 March 1994

Abstract. We have developed a new method to investigate the importance of the propagation of sunlight through the Earth's atmosphere in modelling the perturbations due to radiation pressure from Earth–reflected sunlight — the so–called *albedo effect*. The atmosphere is considered as a refractive optical medium, where Rayleigh scattering takes place. Our mathematical formulation is based on the theory developed in Vokrouhlický et al. (1993c), which allows us to model in a realistic way a number of subtle phenomena. Contrasting with direct solar radiation pressure, which is fairly sensitive to atmospheric processes during the penumbra phases, the albedo effect turns out not to be affected significantly by the atmospheric processes considered here. We have also reinvestigated the behaviour of the radiation specularly reflected from the Earth's surface, and confirm by an independent approach the validity of previous simple models of the corresponding radiative force, provided a "dilution factor" related to the Earth's sphericity and introduced by Wyatt (1963) and later on by Barlier et al. (1986) is properly accounted for.

Key words: celestial mechanics – artificial satellites, space probes – atmospheric effects

1. Introduction

Perturbations of artificial satellite orbits by radiative forces have been studied extensively in the recent past (for reviews, see Milani et al. 1987; Mignard et al. 1990; Vilhena de Moraes 1994). An approximation commonly made in these studies is that of neglecting the optical properties of the medium in between the radiation source(s) and the satellite. Simply speaking, the perturbing photons are assumed to move on straight lines, conserving the radiative intensity transported along the rays. Moreover, the Sun is usually considered as a point–like source of radiation at infinite distance, giving rise to a homogeneous radiative field. These approximations are justified not only by the small magnitude of the radiative perturbations (with respect to the main gravitational forces), but also by the fact that the interplanetary medium is indeed optically extremely thin. The only exception is the Earth's atmosphere, which may even be locally thick.

It is rather interesting that the Earth's atmosphere, being geometrically a very thin layer covering the Earth's surface, can contribute non–negligible effects in the context of the radiative forces. This can be illustrated by two well known examples.

First, we can mention the penumbra effects which determine the direct solar radiation pressure when the satellite crosses the transition region between full sunlight and the Earth's shadow. We have shown in two previous papers of this series (Vokrouhlický et al. 1993c, 1994) that atmospheric effects play a dominant role in the structure of the Earth's penumbra. Actually, this result is not new. It was known at the beginning of the 1960's (e.g., see Link 1962), and taken into account in a number of studies of lunar eclipses (Link 1969). The penumbra phenomena have direct consequences for the instantaneous measurement of non–gravitational perturbations during accelerometric experiments (e.g. Peřestý & Sehnal 1992; Vokrouhlický 1994), and can also give rise to detectable long–term perturbations for satellites whose orbit is tracked with very high accuracy (Vokrouhlický et al. 1994).

Second, the optical properties of the Earth's atmosphere influence the perturbations due to Earth–reflected radiation pressure, commonly referred to as the *albedo effect*. Large cloud formations cause significant local increases of the effective albedo (Taylor & Stowe 1984; Vokrouhlický & Sehnal 1993; Vokrouhlický et al. 1993a). This phenomenon brings about marked features in the resulting albedo force, which may be detected *in situ* by means of accelerometric measurements (Vokrouhlický & Sehnal 1993).

In this paper, we intend to continue our analysis of the influence of atmospheric optics on the radiative forces (Vokrouhlický et al. 1993c, 1994), focusing on the albedo effect. We will not

Send offprint requests to: D. Vokrouhlický (Prague address)

deal with the local variations of atmospheric optical properties (cloud cover, etc.), but rather with the global properties of the atmosphere, seen as a spherically stratified refracting, absorbing and scattering medium. In other words, we will describe the average optical properties of the atmosphere by modelling just the geometry of the rays (refraction) and the physics of the interaction of light with a gaseous medium (absorption, single scattering). As a consequence, near the Earth's shadow edges the counterpart of the penumbra phenomena analysed in Vokrouhlický et al. (1993c) will be shown to play a role in the context of the albedo effect. Our approach treats in a consistent way the illumination of the Earth's surface and the radiation flux on the satellite.

The potential importance of the specularly reflected radiation for the albedo effect has been an open question for a long time. Interestingly, some of the earliest approaches to the albedo effect considered models somewhat in between the specular and diffuse reflection modes (e.g. Levin 1962). This choice was however criticised by Wyatt (1963) and others, who argued that the dominant part of the reflected sunlight acting on satellites is that diffused by the Earth's surface. Later on, refined models of the albedo perturbation were developed, taking into account diffuse reflection only (e.g. Baker 1966; Rubincam & Weiss 1986; Borderies & Longaretti 1990). Some renaissance of interest for the specularly reflected radiation took place during the 80's, when more complex models of the albedo effect were required to understand the orbital evolution of laser–tracked satellites (e.g. Anselmo et al. 1983; Barlier et al. 1986; Rubincam et al. 1987; Vokrouhlický et al. 1993b).

Another purpose of this paper is to clarify some important details of the models for the perturbations arising from specular reflection. As we shall see, a crucial role is played by a simple but fairly subtle correcting factor devised originally by Wyatt (1963) and later reintroduced by Barlier et al. (1986) — in the terminology of the latter paper, the $J(\theta)$ geometrical factor accounting for the dilution of reflected radiation due to the sphericity of the Earth's surface. The omission of this term would lead indeed to considerable errors. We will confirm the validity of the approach of Barlier et al. by a conceptually more fundamental argument, derived from the basic definitions introduced when evaluating the radiative flux integral. In our approach, we split the flux evaluation problem into various steps, the first of which is finding out the geometry of all the rays constituting the radiative field at the satellite position. Therefore, we avoid using the above–mentioned factor $J(\theta)$, as the ray geometry intrinsically contains the information about the dilution of the radiative field reflected from the convex Earth's surface. The confirmation that the method based on the $J(\theta)$ factor provides a good approximation is important, as it also confirms the validity of the results of our previous studies of the albedo long–term perturbations for LAGEOS, where the dilution factor was used (Barlier et al. 1986; Vokrouhlický et al. 1993a,b).

As we shall see, contrasting with the behaviour of the direct solar radiation pressure, the atmospheric effects contribute in a negligible way to the albedo effect. This can be shown most convincingly by adopting two simple extreme models for the optical properties of the Earth's surface: either a constant–albedo, purely diffusive surface or a global mirror causing only a specular reflection. Also, we shall assume a simple spherical shape of the satellite. However, the latter simplifying assumption can be easily generalized by our formalism (at least numerically; see e.g. Vokrouhlický et al. 1993a), and more complex satellite shapes can also be dealt with in a straightforward way.

The remainder of this paper is organized as follows. In Sect. 2 we shortly review the mathematical technique used throughout this series of papers (Vokrouhlický et al. 1993c, 1994) and then derive a precise formulation for the diffuse and specular reflection from the Earth's surface, taking fully into account the main atmospheric effects. In Sect. 3 we apply the theory in the case of the LAGEOS satellite, though the results derived there are valid also for a wider variety of spacecraft. The main conclusions are summarized in Sect. 4.

2. A new approach to the albedo effect

2.1. Summary of the mathematical technique

Throughout this paper we employ the mathematical formalism introduced in Vokrouhlický et al. (1993c). Here we shall just give a summary in order to allow the reader uninterested in the details to understand the main arguments.

The (scalar) radiative flux is usually the essential quantity needed to model the radiative forces. However, in our approach we found more convenient to use the vector quantity $\boldsymbol{F}$ [see Eq. (2)] — which we call *vector flux*. The scalar radiative flux, defined as the energy flowing per unit time through a unit surface area with a given orientation, can be derived from $\boldsymbol{F}$ for an arbitrary orientation of the surface by mean of a simple projection of $\boldsymbol{F}$ on the surface normal (Vokrouhlický et al. 1993c). The vector flux at a given position is determined from two fundamental physical entities: (i) the radiative intensity I, and (ii) the optical rays. The optical rays represent in a sense the guidelines along which the radiative field is transported starting from the radiation sources, while the intensity I conveys all the information about the properties of the radiation field at a local level (it is directly related to the photon distribution function; see e.g. Mihalas 1970). It should be understood that *a priori* one knows the radiative intensity at the sources only (in our case, on the solar photosphere), and not everywhere in the space. To determine I everywhere outside the sources, one has to solve for it from a propagation model. This is very simple if the radiation propagates in the vacuum, but can be relatively involved when the Earth's atmosphere, a rather complex optical medium, is taken into consideration.

The key point of our study is therefore that we have first to find out the properties of the radiative field near the satellite, and only then to compute the radiative force. The essential tool for finding the optical rays is the Fermat principle, while the tool for transporting the radiative intensity along the rays is the radiative transfer equation (see Vokrouhlický et al. 1993c). The solution of these two problems for the particular case of the

sunlight reflected from the Earth's surface is the main issue of this paper.

After having constructed the radiative field $I(\theta,\phi)$ at the position of the satellite, we can apply some simple rules for computing the radiative force acting on the satellite itself. We recall that in the case of a spherical satellite with quasi–isotropic surface optical properties (see Borderies & Longaretti 1990; Vokrouhlický et al. 1993a), the radiation pressure causes an acceleration given by

$$\boldsymbol{a} = \frac{A}{mc}\mathscr{C}_{\mathrm{R}}\boldsymbol{F}\,, \tag{1}$$

where A is the satellite's geometrical cross–section, m its mass, c the velocity of light, $\mathscr{C}_{\mathrm{R}}$ a dimensionless coefficient depending on the satellite's surface optical properties, and the vector flux is defined as

$$\boldsymbol{F} = \int_{(\theta,\phi)} d(\cos\theta)d\phi\; \boldsymbol{n}(\theta,\phi)\, I(\theta,\phi)\,. \tag{2}$$

Let us point out, however, that the construction of the radiative field and the computation of the radiative force are conceptually well separated problems. As a consequence, the method applied in this paper can be applied as well to the case of satellites with complex shapes, provided Eq. (1) is replaced by somewhat more general formulae (given in Vokrouhlický et al. 1993a).

A rather good model of the Earth's atmosphere (i.e., its refractive and physical properties) is crucial in our treatment. No planar model can be applied here, as it would no longer be valid for large zenith angles. Basically, we adopt Garfinkfel's (1944, 1967) model of the atmosphere, neglecting the upper isothermal layer and taking into account only the polytropic, bottom layer, which is the most important as far as optical effects are concerned (this entails typical errors on refraction angles of the order of 5 arcsec only; see the example given by Garfinkel 1967). As the complete theory is thoroughly described in Garfinkel (1967), we do not repeat here a number of rather complicated formulae appearing in it. Let us just sketch out its most important features:

- the atmospheric medium has a polytropic equation of state, with a polytropic index n;
- the refractive index κ of the atmosphere is assumed to follow the Gladstone–Dale relation (i.e., it is linearly dependent on the air density), and its variation with altitude is given by

$$\kappa(h) = 1 + \alpha\left(1 - 2\gamma^2\frac{h}{R_\oplus + h}\right)^n,$$

$$2\gamma^2 = \frac{g_0 R_\oplus}{(n+1)\mathscr{R}T_0}\,,$$

  where $\mathscr{R}$ is the gas constant and g_0 is the gravity at the surface of the Earth;
- the model parameters, playing the role of boundary conditions at the Earth's surface, are the following ones: pressure p_0, temperature T_0, temperature gradient T_0', humidity (water vapor pressure) p' and refractive index $\kappa_{\mathrm{s}} = (1+\alpha)$.

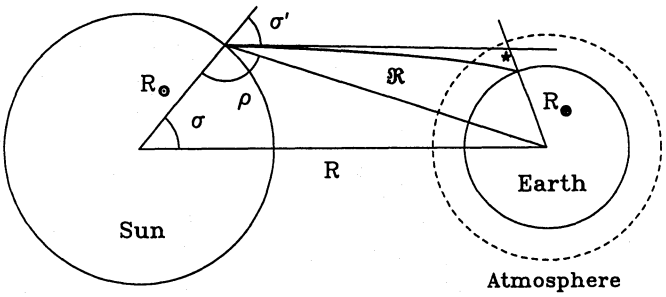

Fig. 1. Geometrical quantities introduced in the text. The solar ray is denoted by $\mathscr{R}$. The last two of Eqs. (5) can be easily derived by noting that the angle marked by an asterisk is just $\pi - z - \mathrm{Re}(z)$

Starting from these quantities, Garfinkel determined the refraction angle (i.e., the difference between the true and apparent ray direction) $\mathrm{Re}(z)$, where z is the apparent zenith distance. [Note that here we define $\mathrm{Re}(z)$ as the refraction angle for the apparent zenith distance z measured on the Earth surface, whereas in our previous two papers (Vokrouhlický et al. 1993c, 1994) we were interested in the refraction angles of the solar rays grazing the atmosphere at some given altitude.]

A suitable choice of the reference systems is important for modelling the albedo effect (see Borderies & Longaretti 1990). We proceed as follows. The satellite's orbit (and consequently the satellite position) is referred to the fixed (inertial) system (X,Y,Z), where the X–axis is directed to the vernal equinox for some given epoch and the Z–axis is close to the Earth's rotation axis. In the (X,Y,Z) frame we define spherical coordinates (Θ,Φ) in the usual way ($X = R\sin\Theta\cos\Phi$, etc.). In order to simplify the integration of the radiative flux (2) at the satellite's position, we introduce a geocentric, satellite–oriented frame $(x_{\mathrm{s}}, y_{\mathrm{s}}, z_{\mathrm{s}})$, with the z_{s}–axis directed to the instantaneous satellite's position, and the x_{s}–axis parallel to local frame's unit vector $\boldsymbol{e}_\Theta$ at the satellite's position.

2.2. *Solar radiative flux at the Earth's surface*

In this section we consider the following problem: given an illuminated Earth's surface element, how much radiative energy flows out of it per unit of time? that is to say, what is the projection $F_\perp$ of the vector flux $\boldsymbol{F}$ on the normal to the surface element? If we assume isotropic diffusion of sunlight (according to Lambert's law) from a surface element of albedo $\mathscr{A}$, the radiative intensity I_{e} emitted towards an arbitrary direction is

$$I_{\mathrm{e}} = \mathscr{A}\frac{F_\perp}{\pi}\,, \tag{3}$$

A common approach (e.g. Rubincam & Weiss 1986; Borderies & Longaretti 1990) is a purely geometrical one, neglecting the atmospheric effects and expressing $F_\perp$ just through the solar constant ($\mathscr{F}$) and the cosine of the local solar zenith angle ($\cos\vartheta_\odot$), that is: $F_\perp = \mathscr{F}\cos\vartheta_\odot$. On the other hand, our approach requires that we express the normal radiative flux $F_\perp$

in Eq. (3) through the projection on the local normal direction of the integral (2). The latter can be computed in a local system bound to the Earth's surface (x_e, y_e, z_e), defined as follows: the z_e axis is normal to the surface and the the x_e axis lies in the plane containing the geocentric position vector of the element and the geocentric Sun–directed unit vector (in fact, this reference frame is close to the solar–oriented frame used in Vokrouhlický et al. 1993c, 1994). In this local frame we can define the polar angles (z, ϕ_z), where z is the usual notation for the apparent zenith angle. Then, the quantity $F_\perp$ can be written as

$$F_\perp = \int_{(z,\phi_z)} d(\cos z) d\phi_z \ \cos z \, I(z, \phi_z) \ . \tag{4}$$

We are going to follow the method developed in Vokrouhlický et al. (1993c): first, we will solve the ray geometry problem in the $\phi_z = 0$ "slice"; next, we will show how this solution can be generalized to other slices $\phi_z = \text{const} \neq 0$, simply by rescaling the solar distance, the solar radius and the Sun–satellite geocentric angular distance. The reader is referred to Vokrouhlický et al. (1993c) for the details. Making use of the first integral of Euler's variational equations resulting from the Fermat principle for a given ray in the atmosphere (see Garfinkel 1944, 1967) and of trigonometric relationships in the triangles shown in Fig. 1, we get the following set of equations:

$$\begin{aligned} \alpha_1 \sin\rho &= \sin(\rho + \sigma) \ , \\ \alpha_2(z) \sin\rho &= \sin\sigma \sin\left(\rho + \sigma'\right) \ , \\ \sigma' &= \sigma - \xi \ , \\ \xi &= z + \mathrm{Re}(z) - \omega \ , \end{aligned} \tag{5}$$

where ω is the geocentric angular distance between the solar centre and the considered Earth's surface element,

$$\alpha_1 = \frac{R_\odot}{R} \quad , \quad \alpha_2(z) = \kappa_s \left(\frac{R_\oplus}{R}\right) \sin z \ , \tag{6}$$

R, $R_\odot$ and $R_\oplus$ are the Earth–Sun distance, the solar radius and the Earth's radius, respectively, and the quantities ρ and σ' are defined geometrically in Fig. 1.

The set of Eqs. (5) is essential in the developments which follow. We can use (5) to solve for σ' provided z is known (this can be called the individual ray problem). This problem has to be solved, when one wants to determine the radiative intensity of the ray characterized by the apparent solar zenith angle z. This quantity can be determined once one knows σ' (through a solar limb darkening model) and the optical path in the atmosphere (whenever the physical interaction of the radiation with the atmosphere is taken into account — see below). As for the solar limb darkening, we use the second Eddington approximation for a grey atmosphere as in our previous papers (Vokrouhlický et al. 1993c, 1994; for a derivation, see Mihalas 1970). Rearranging Eqs. (5), we obtain

$$\cos\sigma' = \cos\left[\arcsin\left(\frac{\alpha_2 - \sin\xi}{\alpha_1}\right)\right] \ . \tag{7}$$

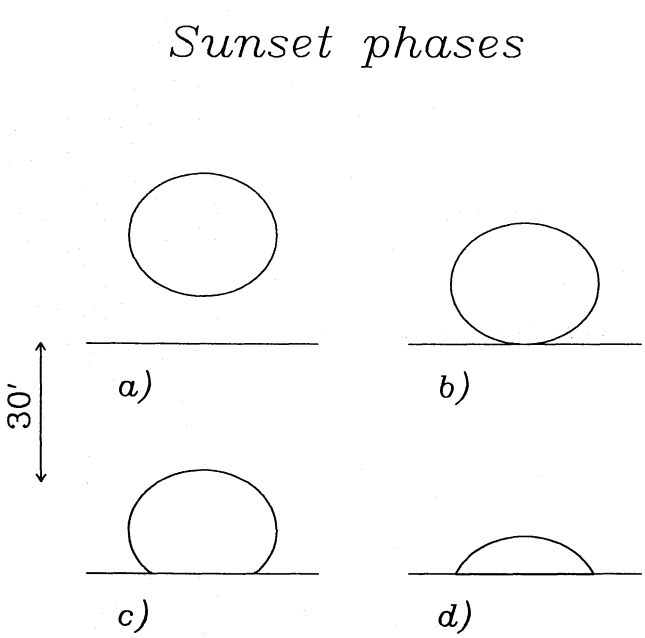

Fig. 2a–d. Sequence of images of the solar disk seen from the Earth's surface during the sunset, according to the individual ray theory of Sect. 2.2. No significant compression of the solar disk shows up, and its vertical width at the beginning of the sunset [image **b**] is about 26 arcmin, in agreement with measurements (Allen 1976)

However, solutions of (5) can be searched for also when other quantities are known. Thus, the values $z = z_\pm$ corresponding to $\sigma' = \frac{\pi}{2}$ give the limits of the solar disk in the local frame's zenith distance. In this case, the equation

$$\eta\xi(z) = \arccos\left[\alpha_1 - \eta\alpha_2(z)\right] - \frac{\pi}{2} \tag{8}$$

has to be solved iteratively for $z_\pm$, where $\eta = \pm 1$ corresponds to the minimum ($\eta = 1$) and maximum ($\eta = -1$) zenith angles of the solar disk.

Finally, setting $z = \frac{\pi}{2}$ and $\sigma' = \frac{\pi}{2}$ or $\sigma' = 0$, we can determine the solar disk visibility from the chosen element of the Earth's surface. Denoting

$$\omega_1 = \mathrm{Re}_\star + \arccos(\alpha_1 + \alpha_2) \ , \tag{9}$$

$$\omega_2 = \frac{\pi}{2} + \mathrm{Re}_\star - \arcsin\left(\frac{\alpha_{2\star}}{\sqrt{1 - \alpha_1^2}}\right) \ , \tag{10}$$

$$\omega_3 = \pi + \mathrm{Re}_\star - \arccos(\alpha_1 - \alpha_2) \ , \tag{11}$$

we consider the following phases: (i) for $\omega < \omega_1$, the whole solar disk as seen from the chosen surface element is above the local horizon; (ii) for $\omega_1 < \omega < \omega_2$, more than half of the solar disk is visible; (iii) for $\omega_2 < \omega < \omega_3$, less than half of the solar disk is visible; and (iv) for $\omega > \omega_3$, the solar disk is completely invisible from the considered location on the Earth. The refraction angle for an Earth–grazing ray ($z = \frac{\pi}{2}$) is $\mathrm{Re}_\star$. The meaning of the quantity $\alpha_{2\star}$ will be given later in this Section.

Figure 2 shows a typical sequence of solar images for increasing values of ω, corresponding to various sunset phases. The sunset starts when the Sun touches the local horizon (case

b). The vertical width of the solar disk is then approximately 26 arcmin, depending on the atmospheric conditions. Compared with a similar sequence of solar images seen from the LAGEOS satellite, no significant compression of the solar disk is observed when the horizon is approached. (See Fig. 4 of Vokrouhlický et al. (1993c), and the explanation given thereof.)

As for the situation when $\phi_z = \text{const} \neq 0$, it can be seen by simple but lengthy algebraic manipulations that the previous solution still holds provided the solar distance (R), its radius ($R_\odot$) and the Sun–satellite geocentric angular distance are rescaled according to the following rules (Vokrouhlický et al. 1993b):

$$R_\odot(\phi_z) = R_\odot \left[1 - \alpha_1^{-2} \sin^2\phi_z \sin^2\omega\right]^{1/2} , \tag{12a}$$

$$R(\phi_z) = R \left[1 - \sin^2\phi_z \sin^2\omega\right]^{1/2} , \tag{12b}$$

$$\cos\omega(\phi_z) = \frac{\cos\omega}{\left[1 - \sin^2\phi_z \sin^2\omega\right]^{1/2}} . \tag{12c}$$

The previous individual ray solution [Eq. (7)] is also valid provided the coefficients α_1 and α_2 [given by Eqs. (6)] are redefined using $R_\odot$, R and ω rescaled according to Eqs. (12). Note that the cosine of the departure of the ray from the normal to the solar surface element, to be used in the solar limb darkening law, is no longer just $\mu_{ss} = \cos\sigma'$, but rather

$$\mu_{ss}(\phi_z) = \left(1 - \alpha_1^{-2} \sin^2\phi_z \sin^2\omega\right)^{1/2} \cos\sigma'(\phi_z) \tag{13}$$

(here the index 'ss' corresponds to 'solar surface'). In Eq. (10) we have denoted the rescaled α_2 parameter for the maximum value of the local ϕ angle ($\sin\phi_{\max} = \alpha_1 \sin^{-1}\omega$) by $\alpha_{2\star}$. It should also be noted that we do not discuss here in full detail the situation occurring on the Earth's surface very close to the subsolar point. Actually, for $\sin\omega < \alpha_1$ ($\approx 5 \times 10^{-3}$), the ϕ angle can take arbitrary values in its interval of definition $(0, 2\pi)$.

In our approach, we include also a simple treatment of the Rayleigh scattering in the atmosphere. We do not attempt a self–consistent solution of the scattering problem in the atmosphere, but rather model the removal of radiative energy along the considered light ray by single scattering centres, effectively equivalent to an absorption mechanism. Before we deal with this effect, recall that Levin (1962) already pointed out that the factor appearing in the expression for the radiative flux emerging from an Earth's surface element is not simply the cosine of the solar zenith angle. The reason is related to the atmospheric phenomena, in part consisting of a "dilution" of the radiative field (see Vokrouhlický et al. 1993c), but mainly due to scattering and absorption processes. From this point of view, our approach represents a step in the direction recommended by Levin to achieve a more realistic treatment of the albedo effect.

The radiative transfer equation in an absorbing medium is formally solved by

$$I(\tau) = I^{(0)} \exp(-\tau) , \tag{14}$$

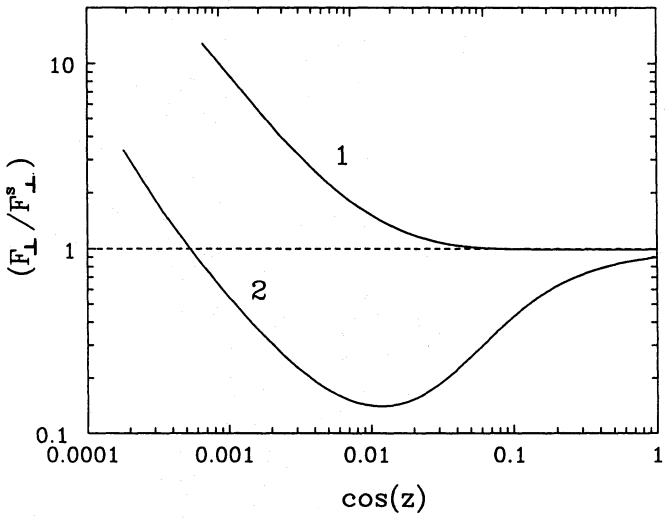

Fig. 3. Normalized scalar radiative flux $\left(F_\perp / F_\perp^s\right)$ (see text) vs. cosine of the zenith angle z of the solar disk's centre. Note that scales are logarithmic on both axes

where $I^{(0)}$ is the ray intensity out of the atmosphere (where it is conserved), and $I(\tau)$ is the ray intensity after an optical path τ in the atmosphere, with

$$\tau = \int ds\, \chi(s) . \tag{15}$$

Here χ is the absorption coefficient and s is the curvilinear abscissa along the ray. Unfortunately, this solution is actually very complex due to the deflection of the ray in the atmosphere. Therefore, we shall neglect the curvature of the path. Were the absorption coefficient constant ($\chi = \chi^\star$) throughout the atmosphere, the integral (15) would have the simple solution

$$\tau^\star = \chi^\star \left[\sqrt{R_\oplus^2 \cos^2 z + h_T\left(2R_\oplus + h_T\right)} - R_\oplus \cos z\right] , \tag{16}$$

for a solar ray characterized by the zenith distance z (h_T is the atmosphere's height). However, the solution (16) would lead to unrealistic results, as the assumption of a constant absorption coefficient is too drastic. We have to assume at least a simple variation of the effective absorption coefficient in the atmosphere, mainly to model its change with the altitude. The effective absorption coefficient due to Rayleigh scattering is at a first approximation a linear function of the atmospheric density (McCartney 1976). Taking into account the properties of Garfinkel's atmospheric model (see Sect. 2.1 above), we can improve the estimate (16) for the optical thickness of the atmosphere in a given local direction z by using instead

$$\tau = \tau^\star \int_0^1 d\zeta \left[1 - 2\gamma^2 \left(1 - R_\oplus \psi^{-1}\left(\zeta;\tau^\star\right)\right)^n\right] , \tag{17}$$

together with

$$\psi\left(\zeta;\tau^\star\right) = \left[R_\oplus^2 + \zeta^2 \left(\frac{\tau^\star}{\chi^\star}\right)^2 + 2R_\oplus \zeta \left(\frac{\tau^\star}{\chi^\star}\right) \cos z\right]^{1/2} ,$$

where $\chi^\star$ is now the absorption coefficient at the Earth's surface (in the examples to be discussed in Sect. 3 we will adopt the numerical value $\chi^\star = 1.162 \times 10^{-5}$ m^{-1}, corresponding approximately to the wavelength $\lambda = 550$ nm. Note that we neglect the dependence of Rayleigh scattering on wavelength.

Summarizing our approach, we can state that every solar ray going through a particular point on the Earth and contributing to the radiative flux integral [Eq. (2)] is assumed to undergo a refractive deflection as described in the first part of this section, while at the same time the radiative intensity carried along the ray is attenuated by a factor $f(\tau^\star; z)\exp(-\tau^\star)$, where

$$f(\tau^\star; z) = \exp\left\{\tau^\star\left[1 - \int_0^1 d\zeta\left[1 - 2\gamma^2\left(1 - R_\oplus\psi^{-1}\left(\zeta;\tau^\star\right)\right)^n\right]\right]\right\} . \qquad (18)$$

Figure 3 shows the dependence of the normal flux $F_\perp$ given by Eq. (4) and normalized to the value without atmosphere, $F_\perp^s = \mathscr{F}\cos\vartheta_\odot$, upon the cosine of the zenith angle z of the solar disk's centre. The two cases without (curve 1) and with (curve 2) Rayleigh scattering have been plotted. The latter curve shows that the flux $F_\perp$ is in general lower than the simple geometric value $F_\perp^s$ owing to attenuation of sunlight, which becomes stronger and stronger as the atmospheric path of the rays gets longer. On the other hand, for very large solar zenith angles (i.e., with the Sun close to the local horizon), refraction yields a significant increase of $F_\perp$ with respect to $F_\perp^s$, due to the well–known phenomenon of the earlier sunrise (and later sunset) caused by the deflection of solar rays. These effects will be further discussed in Sect. 3.

2.3. Albedo radiative flux at the satellite — diffusive Earth's surface

Having solved the problem of the irradiation of an Earth's surface element, we now turn to the analogous problem concerning the irradiation of the satellite from the visible and illuminated Earth's cap. The underlying approach is exactly the same as above: we select all the light rays at the satellite position which are emitted by the Earth's illuminated cap and then we compute, again through Eq. (2), the radiative vector flux, which is directly connected to the perturbing force [Eq. (1)]. In order to perform these computations, we introduce a satellite–centered coordinate frame (x_{sl}, y_{sl}, z_{sl}) (the index 'sl' stands for 'satellite local'), along with the spherical angles (θ_{sl}, ϕ_{sl}). The axes of this frame are parallel to those of the satellite–oriented geocentric frame (x_s, y_s, z_s), and just the origin is moved to the satellite. We cover the source (the Earth's surface cap visible from the satellite) by a suitable grid defined in the satellite–oriented frame introduced earlier (see Fig. 4).

As noted earlier, the individual ray problem (i.e., finding the geometry of a particular ray) is at the heart of our method. Using

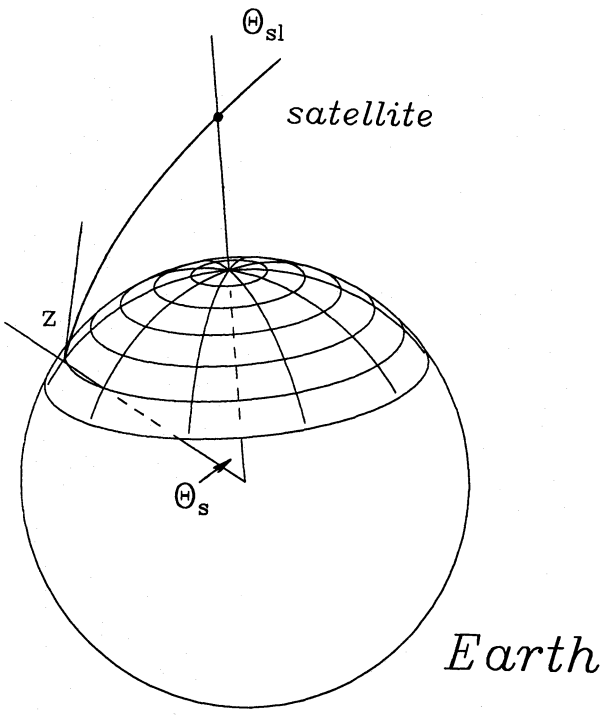

Fig. 4. Coordinates introduced in Sect. 2.3. The Earth's cap visible from the satellite is parametrized by the satellite–oriented angles (θ_s, ϕ_s). The apparent zenith angle of the satellite in the surface element's local frame is z and the spherical angle of the emitter in the satellite–centered frame is θ_{sl}

again the first integral of the variational equations coming from the Fermat principle, we obtain the following set of equations

$$\sin\theta_{sl} = \kappa_s\left(\frac{a}{r}\right)\sin z , \qquad (19a)$$

$$\theta_s = z + \mathrm{Re}(z) - \theta_{sl} , \qquad (19b)$$

$$\phi_{sl} = \phi_s , \qquad (19c)$$

where z is the zenith distance of the selected ray in the local frame of the Earth's surface emitter. Equations (19) can be used as follows: (i) the selected ray is specified by (θ_{sl}, ϕ_{sl}); (ii) then one can solve for the corresponding zenith distance z by means of Eq. (19a); (iii) finally the position of the Earth's surface emitter (θ_s, ϕ_s) can be determined by means of Eqs. (19b,c). Of course, one has to check whether the point is illuminated by the Sun. If atmospheric absorption is neglected, the radiative intensity along the ray is given by Eq. (3), where the normal flux $F_\perp$ refers to the illumination of the surface element characterized by parameters (θ_s, ϕ_s); if on the contrary Rayleigh scattering is taken into account, the intensity becomes

$$I(\theta_{sl}, \phi_{sl}) = \mathscr{A}\frac{F_\perp}{\pi} f(\tau^\star; z)\exp(-\tau^\star) \qquad (20)$$

where $f(\tau^\star; z)$ and $\tau^\star$ are given by Eqs. (16) to (18).

2.4. Albedo radiative flux at the satellite — specular Earth's surface

Our approach to the albedo effect problem can also be used with the assumption that the sunlight is specularly reflected on the surface of the Earth. Of course, this is a more acceptable assumption for the seas than for the continents (Barlier et al. 1986). It turns out that the specularly reflected radiation accounts only for a minor fraction of the Earth's energetic output. However this minor component plays an important role in the perturbations of the motion of LAGEOS (Vokrouhlický et al. 1993b). We stress that by "specular reflection" here we mean ideal reflection of electromagnetic plane waves on the flat boundary between two optical media (air/water in our case). The reflectivity (i.e., the fraction of incoming energy carried away by reflected waves) can be simply evaluated under the assumption of unpolarized ("white") illumination by

$$\mathscr{R}(z) = \frac{1}{2}\frac{\sin^2(z-z_\star)}{\sin^2(z+z_\star)}\left[1+\frac{\cos^2(z+z_\star)}{\cos^2(z-z_\star)}\right] \tag{21}$$

(Jackson 1962), where the refraction angle $z_\star$ is defined by $\varrho \sin z = \sin z_\star$, with $\varrho = 0.7446$ for an air/water boundary.

As for the geometry of the ray, we only have to put together the results of the two previous Sections. In other words, the illumination of each Earth's surface element is treated in the same manner as in Sect. 2.1. In contrast with what occurs in the case of diffuse reflection (Sect. 2.2), when every surface element visible from the satellite can send light rays to it, here we must consider only the points on the Earth's surface which connect the sun and the satellite by specular reflection. Thus, here we treat the Earth's surface as an ideal spherical mirror, with Fresnel–type optical behaviour, and consider the action on the satellite of just the radiation reflected in this fashion. For this purpose, we have to find out those rays, which form a solar image on this "giant mirror", as seen from the satellite. We shall discuss how this can be done in the $\phi_{sl} = 0$ slice, after which the same treatment can be applied to other slices provided the rescalings discussed in Sect. 2.2 are performed. The central point consists in putting the sum $(\omega + \theta_s)$ [from Eqs. (5), (12) and (19)] equal to Ω, that is the geocentric angular distance between the Sun and the satellite.

Suppose that we have chosen a specularly reflected light ray (specified by some value of θ_{sl}) in the satellite–centered local frame. To obtain the radiative intensity of this ray, we first determine the position of the Earth's surface element where the reflection takes place in the satellite–oriented frame (i.e., the corresponding value of θ_s) by using Eq. (19b), and the zenith angle of the reflected ray z by Eq. (19a), that is

$$\sin z = \kappa_s^{-1}\left(\frac{r}{a}\right)\sin\theta_{sl} \,. \tag{22}$$

The cosine of the deflection of the ray from the local normal when it is emitted at the solar surface is then determined by Eq. (7), where we use: (i) the same zenith angle z for the reflected ray as for the corresponding ray incident on the Earth's surface element, as determined from Eq. (22), consistently with the assumption of mirror reflection; (ii) $\omega = \Omega - \theta_s$ for the geocentric angular distance between the reflecting Earth's surface element and the Sun. Denoting by $I_{em}(\mu_{ss})$ (with $\mu_{ss} = \cos\sigma'$) the radiative intensity of the ray when emitted at the solar surface, derived from the solar limb darkening model, we conclude that the radiative intensity of the specularly reflected ray is given by

$$I = \mathscr{R}(z) I_{em}(\mu_{ss}) \,, \tag{23}$$

when the atmospheric scattering is neglected, or by

$$I = \mathscr{R}(z) f^2(\tau^\star; z)\exp(-2\tau^\star) I_{em}(\mu_{ss}) \,, \tag{24}$$

when Rayleigh scattering is accounted for [with $\tau^\star$ given by Eq. (15)]. Note the square of the altitude correction factor $f(\tau^\star; z)$ in Eq. (24), due to the fact that the ray crosses twice the Earth's atmosphere.

As we did earlier, the equations expressing the geometry of individual rays can be solved inversely to find out which satellite local directions correspond to sunlight specularly reflected on the Earth. After some rearrangements of Eqs. (8) and (19a,b), we obtain the following set of equations:

$$z + \mathrm{Re}(z) + \omega = \Omega + \arcsin\left[\kappa_s\left(\frac{a}{r}\right)\sin z\right] \,, \tag{25a}$$

$$z + \mathrm{Re}(z) - \omega = \eta\left[\arccos\left(\alpha_1 - \eta\alpha_2(z)\right) - \frac{\pi}{2}\right] \,, \tag{25b}$$

which has to be solved for z and ω. Here again $\eta = \pm 1$ corresponds to the lowermost and uppermost rays specifying on the chosen ϕ_z–slice the limits of the solar disk image.

3. Albedo effect perturbations

Although here we restrict the discussion to the perturbations on the satellite LAGEOS, very similar results would be found for other satellites (in both low and high Earth orbits — in particular we examined the case of MACEK accelerometric spacecraft, see Vokrouhlický 1994). In order to simplify the geometry and to derive upper limits for the effects to be analyzed, we have slightly modified the real LAGEOS' orbit. We have put the Sun on the Earth's equatorial plane, in the same direction as the instantaneous ascending node of the orbit. Moreover, we have assumed a polar orbit, namely a 90° inclination instead of the $\approx 110°$ inclination of the real orbit. This simplified geometry has already been used in previous studies of the albedo effect on LAGEOS (Rubincam et al. 1987; Lucchesi & Farinella 1992), so that it will be possible to compare our results with previous ones. As for the coordinate grids needed for the numerical evaluation of the flux integrals, we adopted: (i) a 51×51 grid for the flux of sunlight through the Earth's surface elements (Sect. 2.2); (ii) a 61×61 grid for the flux of sunlight diffused from the Earth (i.e., on the Earth's cap visible from the satellite, see Sect. 2.3). The corresponding grid spacings have been tested to be small enough to guarantee the numerical accuracy of the results. We also chose a fairly short step in LAGEOS' orbital mean anomaly — about 5 s in time — in order not to miss subtle penumbra phenomena (we recall that LAGEOS' orbital period is 13,540 s).

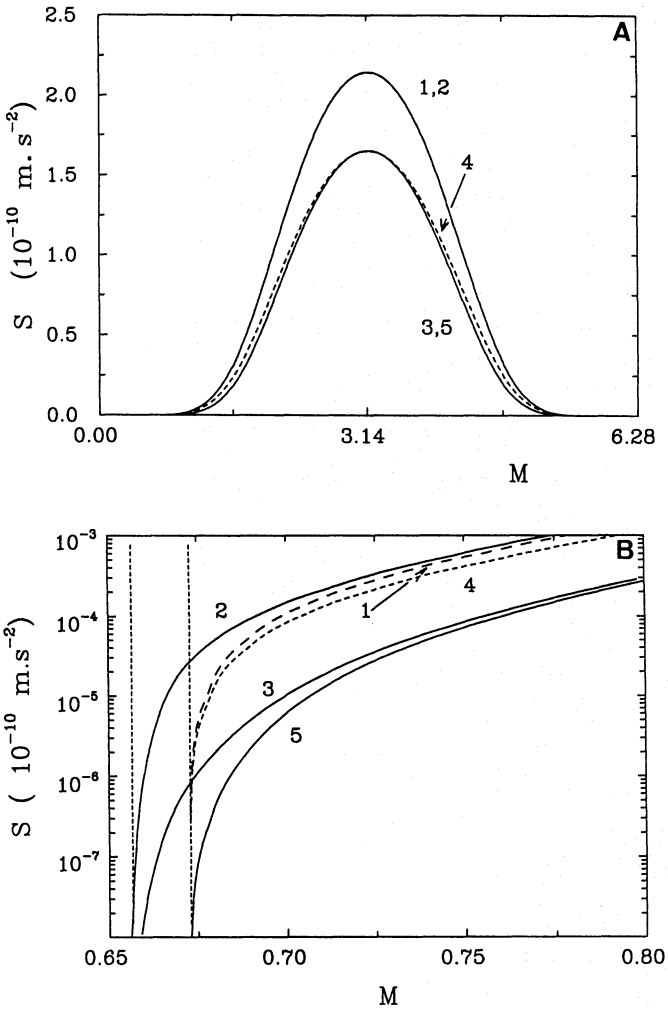

Fig. 5a and b. The radial [part **a**] component of the albedo perturbation along LAGEOS' modified orbit (as described in the text) vs. orbital mean anomaly. Here the Earth is considered as an ideal Lambertian diffusor with constant albedo $\mathscr{A} = 0.25$. The dashed curve 1 corresponds to the simple model neglecting all the atmospheric phenomena, the solid curve 2 to the model accounting for atmospheric refraction only (no scattering; note that both curves coincide at the scale of this plot), the solid curve 3 to the model accounting also for Rayleigh scattering with altitude–dependent absorption coefficient. Part **b** enlarges the short transition phase when the satellite leaves the Earth's shadow (the dashed region corresponds to the penumbra phase). Here curves 1, 2 and 3 are the same as in part **a**, but now the pair of curves 1 and 2 (as well as the pair 4 and 5), can be seen independently. Curve 4 corresponds to the atmosphere–free model, but rescaling the albedo value to $\mathscr{A} = 0.193$. Curve 5 corresponds to a combination of the simpler and the more accurate approaches: the ray geometry is treated as in the atmosphere–free case (straight lines), but simultaneously the Rayleigh scattering factor (18) is used

The optical thickness of the atmosphere due to molecular scattering at $\lambda \approx 550$ nm is known to be $\tau \approx 0.096$ (see Allen 1976). Applying Eq. (17) for the altitude correction factor and putting $z = 0$ to get the optical thickness in the zenith direction, we obtain $\tau_{\text{vert.}} \approx 0.094$, in good agreement with the above–mentioned value. Near the local horizon (i.e., for $z = \frac{\pi}{2}$), the optical thickness is considerably larger, since the rays perform a longer path through the atmosphere, essentially in the lower layers where the density is higher. From our formulae we obtain $\tau_{\text{horiz.}} \approx 3.3$, or equivalently an attenuation of the intensity of $\approx \exp(-3.3) \approx 0.037$. This is again in good agreement with the extrapolation of data given by Siedentopf & Scheffler (1965).

The strong sensitivity of the attenuation with the zenith distance has interesting implications. On one hand, a strong attenuation decreases the magnitude of the albedo force on the satellite. On the other hand, both the Earth's cap visible from the satellite and the fraction of the Earth's surface illuminated by sunlight become larger as a result of atmospheric refraction, which in turn tends to increase the magnitude of the albedo force. The competition between the effects of absorption and refraction has the following consequences. First, when the satellite is close to the edge of the Earth's shadow, the larger illuminated and visible region leads to a penumbra–type effect (Vokrouhlický et al. 1993c), characterized by an earlier rise of the albedo force (see Fig. 5b). Second, when the satellite is well above the illuminated part of the Earth's surface, the albedo force decreases since Rayleigh scattering dominates (Fig. 5a). The same mechanisms were also apparent in Fig. 3.

We also tested two approximate models useful in orbital dynamics to save computing time without significant loss of accuracy. First, we have just rescaled the value of the Earth's albedo coefficient defined in the atmosphere–free model, and this leads already to a much better agreement between the results of the model neglecting atmospheric effects and those of the more complex model including both refraction and Rayleigh scattering. In the case shown in Figs. 5 (curve 4), it was sufficient for this purpose to choose $\mathscr{A} = 0.193$ as the effective Earth's albedo instead of 0.25, the "true" value at the bottom of the atmosphere; note that the ratio between the two albedo values is close to the vertical sunlight attenuation in the atmosphere, that is $\exp(-2 \times 0.094)$. An even better agreement is obtained by keeping the Earth's albedo at 0.25 and combining the simple geometrical approach with straight light rays (no refraction) with an effective damping of the radiative intensity by the factor given by Eq. (18). The results of this model are represented by curves 5 in Figs. 5. Apart from the missing penumbra–type effects (see Fig. 5b), the agreement with the reference solution (curve 3) is remarkable.

The force components arising when specular reflection only is considered are plotted in Figs. 6. Only little differences are observed between the simple geometric model based on Barlier's et al. (1986) formulae, including the $J(\theta)$ dilution factor, and our more complex model accounting for the refractive effects only, in spite of the very different mathematical techniques used in the calculations. Actually, apart from the absorption–related rescaling of the albedo coefficient, the atmosphere appears to play just a minor role in the albedo effect, which is amplified only near the shadow edges (see Fig. 6c). The excellent agreement between the results provided by the two approaches is important, and confirms the validity of the rather crude model introduced by Barlier et al. (1986), and based on the use of the $J(\theta)$ "dilution factor" (see Sect. 1).

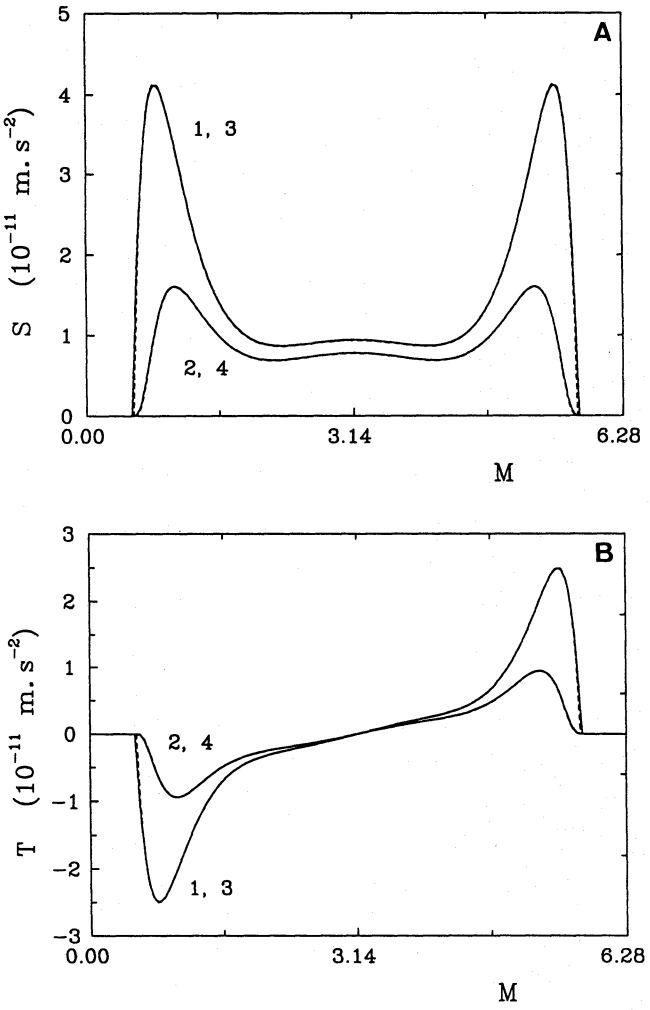

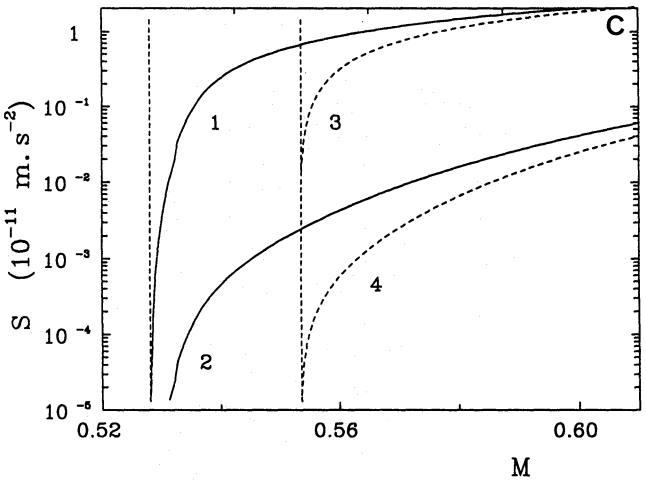

Fig. 6a–c. Radial [part **a**] and transverse [part **b**] components of the albedo acceleration along LAGEOS' modified orbit (see text) vs. mean anomaly (M). Specular Fresnel–type reflection of sunlight from the whole Earth's surface has been assumed. Dashed curves 3 and 4 correspond to the simple geometrical approach of Barlier et al. (1986), whereas solid curves 1 and 2 correspond to the more precise approach developed in this paper. In case 1, only refractive atmospheric effects have been taken into account, while in case 2 Rayleigh scattering with an altitude–dependent absorption coefficient was also accounted for. In case 3 and 4, we assumed no refraction (straight rays), but in case 4 the Rayleigh atmospheric attenuation was accounted for as with case 5 in Figs. 5. The earlier rise of the radial component caused by refraction when the satellite is close to the shadow's edge is displayed in part **c**. Note, however, that this penumbra phase is quite short

Figure 7 shows the apparent shape of the Sun seen from the satellite on the convex Earth's surface, and gives a clear idea of why the simple geometric approach is so successful. Although the Sun is an extended radiative source, its image is very small, owing to the dilution of the reflected radiation (due to the geometry of reflected rays from a spherical mirror). This also shows why in Barlier's et al. approach the use of $J(\theta)$ is essential.

Another important remark is that omission of the Fresnel reflectivity coefficient [Eq. (21)] would lead to considerable errors. The resulting perturbing force would not only be larger in magnitude (by a factor of 10 or more), but would also behave in a qualitatively different way — e.g., there would be only one maximum of the radial force component when the satellite is just above the subsolar point. Therefore, although the instantaneous effect of the specularly reflected radiation is small (even when compared to other nongravitational effects; e.g., for the real Earth it contributes only a minor fraction of the total albedo force), oversimplified modelling of this effect may lead to inaccuracies accumulating during the long–term evolution of the orbit. We stress that a correct treatment of the force due to reflected radiation is not yet commonplace in the dynamical models used in mission planning (see e.g. Antreasian 1992).

Another problem related to the specularly reflected radiation, that we have not analysed in this paper, originates from the fact that the real ocean surface is not a perfect spherical mirror, but usually has complex wave patterns over a wide range of wavelengths (Wyatt 1963). As a consequence, the real image of the Sun as seen from the satellite on the ocean is much fuzzier and larger than those displayed in Fig. 7 — as it can be guessed by looking from a beach at the sunlight reflected from the water before sunset. Qualitatively, the effect of ocean waves can be simulated by assuming that specularly reflected light is spread over a finite–sized cone surrounding the direction predicted by geometric optics (Rubincam et al. 1987; Lucchesi & Farinella 1992). However, this rather complicated phenomenon (see discussion in Bass & Fuks 1979) appears to deserve further study, and we plan to do it in a forthcoming paper.

4. Conclusions

In this paper we have presented a new method to model the albedo effect, namely the perturbing force on Earth satellites due to the sunlight reflected by the Earth. This method allows

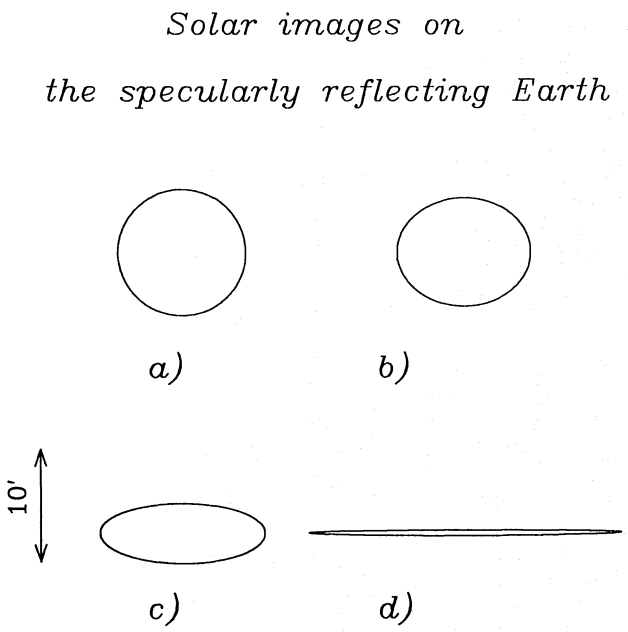

Fig. 7a–d. Sequence of solar disk images seen from the LAGEOS satellite on the specularly reflecting Earth. Case **a** corresponds to the configuration when the subsolar and subsatellite points on the Earth's surface coincide. In this case, the image is circular. Otherwise, the images are "compressed", although the area of all of them is roughly the same. Note also that the images are significantly smaller than the real solar disk, as a consequence of the spherical shape of the Earth's surface

us to investigate in detail the role of the Earth's atmosphere, considered as an isotropic optical medium characterised by uniform refractive and absorptive properties. Our approach deals in a consistent way with the atmospheric effects, both when the illumination of the Earth's surface is considered and when the satellite's irradiation by Earth–reflected sunlight is evaluated. The results can be compared with the more commonly used, simple treatment of the albedo effect neglecting the interaction of light with the atmosphere. In order to better understand these phenomena, we used simplified models of the Earth's optical properties and the satellite's shape, but more realistic models can be easily treated in a similar way.

The influence on the albedo effect of penumbra phenomena, occurring when the satellite is close to the edges of the Earth's shadow, can be realistically modelled in our approach. Compared to the case of the direct solar radiation pressure (Vokrouhlický et al. 1993c), the penumbra phenomena are found here to be much less important, mainly because the solar illumination for large zenith angles results in a very small radiative flux through the corresponding Earth's surface elements [see Eq. (3)], as a consequence of Rayleigh scattering. The influence of sunlight attenuation due to this scattering is quite pronounced (see Fig. 5a). However, we have shown that the details can be neglected, provided a smaller effective value of the albedo coefficient of the planet is adopted.

We have also discussed the effects of the specularly reflected sunlight. Here again, the atmospheric effects do not play an important role. On the other hand, we establish on firm grounds the validity of the approach of Barlier et al. (1986), who correctly accounted for the dilution of the radiative field due to the curvature of the Earth's surface. The omission of the corresponding coefficient would bring significant errors in the force model.

The main limitation of the physical model used in our approach involves the Rayleigh scattering, in both the diffuse and the specular reflection cases. The scattering was not treated in a fully consistent manner, as we took into account only the radiation removed by single scattering on one hand, and did not attempt to model the contribution of scattered light on the other hand. A self–consistent study of the full scattering problem in the context of radiation forces would deserve more attention.

Finally, the reader is reminded that the phenomena studied in this paper should not be mistaken for the influence of the cloud coverage on the Earth's optical properties and the albedo effect. One has to distinguish between the *global* (somewhat averaged) character of the atmospheric optical properties, considered here, and the *local* (and rather erratical) character of the cloud coverage. The influence of local cloud phenomena had been addressed in two previous papers (Vokrouhlický & Sehnal 1993; Vokrouhlický et al. 1993a), and was found to be quite important.

Acknowledgements. We acknowledge helpful remarks by R. Vilhena de Moraes. D.V. was partially supported by the IBM Academic Initiative in the Czech Republic. P.F. worked at this project while staying at the Observatoire de la Côte d'Azur (Nice, France), thanks to the "G. Colombo" fellowship of the European Space Agency.

References

Antreasian, P.G., 1992, Precision radiation force modeling for the TOPEX/POSEIDON mission, Ph. D. Thesis, University of Colorado
Allen C.W., 1976, Astrophysical Quantities, Athlone Press, London
Anselmo L., Farinella P., Milani A., Nobili A.M., 1983, A&A 117, 3
Baker R.M.L., 1963, Radiation on a satellite in the presence of partly diffuse and partly specular reflecting body, In: M. Roy (ed.), Dynamics of Satellites. Springer–Verlag, Berlin, p. 85
Bass F.G., Fuks I.M., 1979, Wave Scattering from Statistically Rough Surfaces, Pergamon Press, Oxford
Barlier F., Carpino M., Farinella P., Mignard F., Milani A., Nobili, A.M., 1986, Ann. Geophys. 4, 193
Borderies N., 1990, Celest. Mech. 49, 99
Borderies N., Longaretti P.Y., 1990, Celest. Mech. 49, 69
Chandrasekhar S., 1950, Radiative Transfer, Oxford University Press, Oxford
Garfinkel B., 1944, Astron. J. 50, 169
Garfinkel B., 1967, Astron. J. 72, 235
Klinkrad H., Koeck Ch., Renard P., 1990, ESA Journal 14, 409
Jackson J.D., 1962, Classical Electrodynamics, J. Willey & Sons, New York
Levin E., 1962, ARS Journal, 1328
Link F., 1962, Bull. Astron. Inst. Czech. 13, 1
Link F., 1969, Eclipse Phenomena in Astronomy, Springer–Verlag, Berlin
Lucchesi D., Farinella P., 1992, J. Geophys. Res. 97, 7121

McCartney E.J., 1976, Optics of the Atmosphere (Scattering by Molecules and Particles), J. Willey & Sons, New York

Mignard F., Afonso G., Barlier F., Carpino M., Farinella P., Milani A., Nobili A.M., 1990, Adv. Space Res. 10, (3)221

Mihalas D., 1970, Stellar Atmospheres, W.H. Freeman and Co., San Francisco

Milani A., Nobili A.M., Farinella P., 1987, Non–Gravitational Perturbations and Satellite Geodesy, A. Hilger, Bristol

Peřestý R., Sehnal L., 1992, In–orbit microaccerelerometric experiment, presented at the 43rd congress of the International Astronautical Federation, Washington DC

Rubincam D.P., Weiss N.R., 1986, Celest. Mech. 38, 233

Rubincam D.P., Knocke P., Taylor V.R., Blackwell S., 1987, J. Geophys. Res. 92, 11,662

Siedentopf H., Scheffler H., 1965, Astronomical instruments: Influence of the Earth's atmosphere, In: Voigt H.H. (ed.), Landolt-Börnstein Numerical Data and Functional Relationships in Science and Technology, Springer–Verlag, Berlin, p. 48

Taylor V.R., Stowe L.L., 1984, J. Geophys. Res. 89, 4987

Vilhena de Moraes R., 1994, Adv. Space Res. 14, (5)45

Vokrouhlický D., 1994, Publ. Astr. Inst. Ondřejov, in press

Vokrouhlický D., Sehnal L., 1993, Celest. Mech. 57, 493

Vokrouhlický D., Farinella P., Lucchesi D., 1993a, Celest. Mech. 57, 225

Vokrouhlický D., Farinella P., Lucchesi D., 1993b, A&A 280, 282

Vokrouhlický D., Farinella P., Mignard F., 1993c, A&A 280, 295 (paper I)

Vokrouhlický D., Farinella P., Mignard F., 1994, A&A 285, 333 (paper II)

Wyatt S.P., 1963, The effect of terrestrial radiation pressure on satellite orbits, In: M. Roy (ed.), Dynamics of Satellites, Springer–Verlag, Berlin, p. 180

This article was processed by the author using Springer-Verlag TEX A&A macro package 1992.